http://dx.doi.org/10.5012/bkcs.2013.34.5.1333

Articles

Chitosan Nanoparticles as a New Delivery System for the *Anti*-HIV Drug Zidovudine

El Montassir Dahmane, Mohammed Rhazi,† and Moha Taourirte*

Laboratoire de chimie Bio organique et Macromoléculaire (LCBM); Département des Sciences Chimiques, Faculté des Sciences et Techniques Guéliz (FSTG), B.P. 549, Marrakech, 40000, Morocco
**E-mail: Taourirte@gmail.com, el_montassirfstg@yahoo.fr*
†Laboratoire des Macromolécules Naturelles (LMN), Ecole Normale supérieure, BP S41, Marrakech, 40000, Morocco
Received December 3, 2012, Accepted February 1, 2013

Chitosan-based nanoparticles (CSNP) were prepared through ionic cross-linking and gelation of chitosan (CS) by tripolyphosphate (TPP). CS properties such as molecular weight, and preparation conditions were screened and the resulting nanoparticles were examined by Fourier transform infrared spectroscopy (FTIR), scanning electron microscopy (SEM) and transmission electron microscopy (TEM). The obtained particles were consistently spherical with an overall diameter of approximately 107 ± 20 nm. They were successfully used as a carrier for Zidovudine, an *anti*-human immunodeficiency virus (HIV) which, to our knowledge, is novel. The encapsulation ability, loading capacity, and controlled release behavior for these CSNP was evaluated. Results indicated that their intrinsic properties were strongly affected by properties inherent to CS such as molecular weight, and by the preparation condition, such as cross-linking density, which depends on the concentration of the cross-linker. *In vitro* release tests for the entrapped zidovudine showed that the CNNP provided a continuous release that can last upwards 20 h.

Key Words : Chitosan, Nanoparticles, Zidovudine, Controlled drug delivery

Introduction

Zidovudine (AZT), a nucleoside analog reverse transcriptase inhibitor, is the first *anti*-HIV drug clinically approved and commercialized. Despite some limitations, it is still, either alone or in combination with other antiviral agents, widely used for the treatment of AIDS and related complexes. The main clinical limitations to the therapeutic effectiveness of AZT are its short plasma half-life (approximately 1 h), necessitating frequent administration of large doses to maintain therapeutic drug levels, and its dose-dependent toxicities.[1-4] In fact, after oral administration, AZT is completely and rapidly absorbed leading to very high initial plasma concentrations and, therefore, a high incidence of toxicity results in frequently occurring side effects. As a result, adequate delivery systems for AZT are still investigated to develop a method to maintain effective plasma concentrations as well as to reduce dose and dose-dependent toxicity.[5] Different strategies and technologies for alternative AZT delivery such as controlled release formulations that help to achieve a maximum therapeutic effect with simultaneous minimization of adverse effects have been recently explored. For HIV/AIDS therapy, nanocarrier platforms are gaining a tremendous amount of attention to enhance preferential delivery of various drugs including AZT, to the cellular and anatomic reservoir sites in order to improve effectiveness as well as patient tolerance[6]. The rationale for the use of such delivery systems is their ability to efficiently encapsulate different types of therapeutic payloads, promote oral absorption, protect against degradation in the systemic circulation and, most importantly, promote efficient delivery and residence in tissues/organs, and allow for intracellular localization.[7] Examples of nanocarrier systems are commonly made of biodegradable polymers and lipids, including nanoparticles, micelles (self-assembled amphipathic polymer molecules), dendrimers (tree-like polymeric structures), liposomes (phospholipids, nanovesicles) and nanoemulsions, *etc*….[6-8] Polymer-based nanoparticles, where the drug is encapsulated within a polymer matrix of nanoparticles having a diameter below 1000 nm (and typically 100-500 nm) have drawn considerable interest in the last several years as nanocarriers for drug delivery. They have been actively investigated for controlled drug delivery for a variety of diseases.[8] They offer numerous advantages, such as small particle size and narrow size distribution, which offers a large surface-area-to-volume ratio for efficient payload encapsulation and delivery. A number of biodegradable polymers have been used for the design of nanoparticulate systems for drug delivery; chitosan, one of these systems, offers a great promise as it is a particularly interesting polymer for the association and delivery of active compounds for different reasons.[9,10] Chitosan, α (1–4) 2-amino 2-deoxy β-D glucan, has structural characteristics similar to glycosaminoglycans. This polycationic biopolymer is generally obtained by alkaline deacetylation of

the largely available renewable resource "chitin", which is the main component of the exoskeleton of crustaceans, such as shrimp.[11] Chitosan possesses many physicochemical and biological properties that promote its recognition as a promising material for biomedical and pharmaceutical applications in general, and more particularly for drug delivery.[12-14] It has interesting biopharmaceutical characteristics such as low toxicity, pH sensitivity, biocompatibility and can be metabolized by certain human enzymes, especially lysozyme.[15] Also, being hydrosoluble and positively charged, chitosan is able to interact with negatively charged macromolecules in contact with surfaces, a property that makes it a very useful polymer for mucosal drug delivery.[16,17] In addition, it possesses excellent permeation enhancing properties[18] that enable the opening of the epithelial tight junctions.[19,20] Therefore, chitosan is extensively used in drug delivery in the treatment of various diseases and the formulations are processed in different shapes to meet the needs and specific requirements of each delivery. Powder, injectable solutions, gels, and more particularly micro/nanoparticles have been designed. Chitosan-based micro/nanoparticles are the most important form of the chitosan-based materials employed in drug delivery.[21,22] They were applied to drug delivery for a wide spectrum of diseases including cancer, cardiovascular diseases, respiratory issues, diabetic, some vaccines, and infectious diseases in the body, among others.[23-30] The purpose of the present work was to create biodegradable nanoparticles based on chitosan and evaluate, for the first time to our knowledge, their potential as carrier for an *anti*-HIV drug, namely zidovudine. These nanoparticles were prepared by gelation of chitosan by ionic cross-linking with tripolyphosphate and characterized in terms of their morphology, association efficiency, and *in vitro* release behaviors.

Experimental

Materials. Sodium tripolyphosphate (TPP), zidovudine (AZT), phosphate buffered saline (PBS), acetic acid and different solvents were obtained from Sigma-Aldrich. All chemicals were of analytical grade.

Preparation of Chitosan Samples. Chitosan (CS) with a degree of acetylation (DA) of 8, 10% and molecular weight (Mw) of 13, 63 and 125 kDa was prepared following a process already optimized in our previous studies.[31,32] Briefly, purified chitin, extracted from wastes of shrimp, was deacetylated according to the procedure reported by Broussignac[33] which consisted of a treatment at 120 °C for 24 h with a solution of potassium hydroxide (50 w/w %) in a mixture of ethanol and monoethyleneglycol. The resulting chitosan samples were then characterized in terms of their DA and Mw. The DA was calculated from ^{1}H-NMR spectra recorded using a Bruker AC300. The samples were dissolved in D2O in the presence of 2% of DCl and the spectra were recorded at 343 K. The DA values were calculated from the ratio of the integral of –CH3 signal at 2.15 ppm to the integral of H-1 protons at 5 ppm according to Lavertu *et al.*.[34] The molecular weights were measured by viscosity and the measurements were performed in 0.3 M aqueous acetic acid/ 0.2 M sodium acetate as solvent and using an Ubbelohde capillary viscometer (Ø=0.5 mm) at 25 °C.[35]

Preparation of Zidovudine Loaded Chitosan Nanoparticles. Unloaded and AZT-loaded CS nanoparticles were prepared by ionic gelation of CS with TPP anions. CS solutions (2.5 mg/mL) were prepared by dissolving it in 0.3 M aqueous acetic acid. After complete dissolution, the desired amount of AZT was added to the solution in order to obtain different concentrations *i.e.* 1, 2 and 4 mg/mL. Similarly, a blank sample was prepared without the addition of AZT. Then 6.25 mL of each AZT-CS solution was added drop wise and under continuous stirring to 2.5 mL of TPP aqueous solution having a concentration of 2.5, 5 or 10 mg/mL to reach weight ratios of TPP to CS (TPP/CS) around 0.4, 0.8 and 1.6 respectively. An opalescent suspension was formed instantaneously. Nanoparticles were then separated by centrifugation at 5,000 rpm at 20 °C for 30 minutes, freeze-dried, and stored at 4 °C until further use.

Fourier Transform Infrared Spectroscopy (FTIR) analyses. FTIR spectra were recorded on a Fourier Transform Infrared Spectrometer (Bruker VERTEX-70) using KBr pellets. Spectra (32 scans at 4 cm^{-1} resolution) were collected in the 4000-400 cm^{-1} range.

Scanning Electron Microscopy Analyses. The morphology of the resulting nanoparticles was observed using scanning electron microscopy (SEM). Samples were coated with graphite under vacuum using an automatic sputter coater. The analyses were conducted using a scanning electron microscope (Quanta 200) operating at an accelerated voltage of 16 kV.

Transmission Electron Microscope (TEM) Analyses. Samples of nanoparticles were prepared from a drop of a dilute nanoparticles suspension in water, which was deposited on a carbon coated copper grid. Excess solution was removed with a filter paper, and let dry by natural evaporation. The sample grid was observed at 120 kV using a Tecnai G2 transmission electron microscope.

Evaluation of Drug Loading Efficiency. The encapsulation efficiency and loading capacity of nanoparticles were determined by separation of nanoparticles from aqueous medium containing free AZT by centrifugation at 5000 rpm for 30 min. The amount of liberated AZT in supernatant we measured by High Performance Liquid Chromatography (HPLC). The HPLC system was equipped with an analytical column (C18 column 100 mm × 4 mm I.D., 5 µm particle size (SGE, Australia)), and an UV detector (Jasco UV-975, Japan) with the wavelength set to 260 nm. A mixture of 20% acetonitrile in 15 mM sodium phosphate buffer (adjusted to pH 7 with sodium hydroxide) was used as eluent at the flow rate of 1 mL/min. Under these conditions, the AZT was eluted at 1.68 min. The AZT loading capacity (LC) of the nanoparticles and AZT encapsulation efficiency (EE) were calculated from Eqs. (1) and (2):

$$LC = A–B/C \times 100 \quad (1)$$

$$EE = A–B/A \times 100 \quad (2)$$

in which A is the total amount of AZT, B is the free amount of AZT in the supernatant, and C is the weight of nanoparticles.

***In vitro* AZT Release.** The AZT loaded nanoparticles were placed into tubes with 1.5 mL of phosphate buffer saline (PBS), and incubated at 37 °C. At varying time intervals, supernatants were isolated by centrifugation and replaced by fresh medium with the same volume (1.5 mL). The amount of released AZT was analyzed with HPLC as described previously. The cumulative release percentage was determined by the following Eq. (3):

$$\text{Drug release } \% = F(t)/F(0) \times 100 \quad (3)$$

in which F(0) and F(t) represent the amount of drug loaded and amount of drug released at a time t, respectively. All tests were done in triplicate.

Results and Discussions

CS is a biologically compatible biopolymer that is chemically versatile since it is found in a variety of forms, differing particularly in molecular weights (Mw) and degree of acetylation (DA). These two basic properties have been used to create a plethora of formulations for diverse applications, mainly in the biomedical field. More importantly, the fact that the DA and Mw of CS can be controlled makes it a material of choice for developing micro/nanoparticles with tunable properties. Free amine groups are readily available for crosslinking, particularly for ionic crosslinking with multivalent anions. This can be straight forwardly performed since the amine groups can undergo protonation under acidic conditions (pH < 6.5), in which the polymer is usually soluble. Tripolyphosphate (TPP) is a typical polyanion that can easily diffuse into CS droplets to form ionic cross-linked CS nanoparticles. Numerous reports have been published on the formation of CS nanoparticles with controlled morphologies based on its crosslinking with TPP. In the present work, we use these polyanions to form CS nanoparticles.

Preparation and Characterization of Chitosan. Polymer's features, mainly Mw and eventually the presence of functionalities and their amount, have a great influence on the final properties of the resulting particles. Therefore, three different molecular weights of CS were prepared and studied in the present work. CS samples were prepared by controlled deacetylation of chitin extracted from shrimp waste. Molecular weights of 13, 63 and 125 kDa were successfully achieved as determined by viscosity measurements, while the targeted DA was set between 8 to 10% as verified by ^{1}H-NMR (spectra not shown here). The resulting CS samples (DA = 8%, Mw = 13, 63 kDa and DA = 10%, Mw = 125 kDa) were used to prepare particles through ionic crosslinking-induced gelation. In addition to varying the molecular weights of the CS, the crosslinking density was also adjusted by varying the concentration of crosslinker in order to fine-tune the morphology of the resulting nanoparticles.

Characterization of Chitosan Nanoparticles. The size and surface characteristics of the nanoparticles are of prime importance in therapeutic applications because they determine their ability to alter biodistribution and pharmacokinetics of drugs. Particles of ~100 nm diameter with hydrophilic surfaces have a longer circulation in blood, especially for injectable delivery, which results in a prolonged duration of drug activity and also an increase in targeting efficiencies to specific sites.[36] After ionic crosslinking and gelation with TPP under different conditions and purification, the resulting CS particles we observed by SEM and an example of recorded images is given in Figure 1.

For a sample of approximately 200 individual nanoparticles in TEM and SEM images (Fig. 1), the average diameters was 107 ± 20 nm. In TEM images, the nanoparticles were mostly present as individual elements because they were dispersed in water. However in SEM images, the nanoparticles were mostly present as aggregates (with some separate individual nanoparticles) because the SEM images were taken directly from lyophilised nanoparticles powder.

The particles were regularly spherical displaying smooth surfaces. Their size distribution was very narrow. Comparable values have been reported for CS-based particles prepared utilizing a similar procedure.[37-39] By varying the concentration

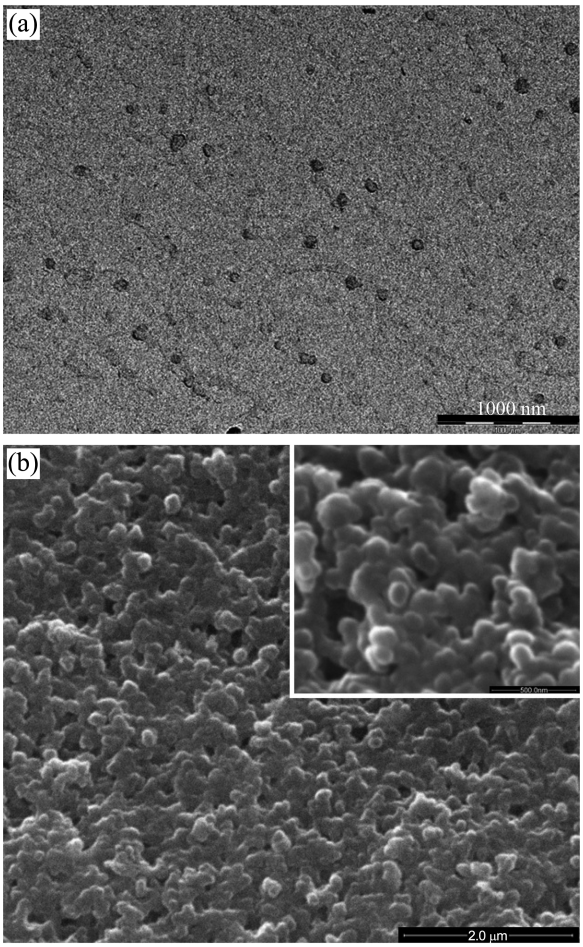

Figure 1. Images of chitosan nanoparticles (Mw = 125 KDa, TPP/CS = 1.6) loaded with AZT (at initial concentration of 1 mg/mL). A (Transmission electron microscopy image), B (Scanning electron microscopy image).

of the crosslinker (TPP/CS ratio), which governed the crosslinking density, a slight decrease of diameter of the nanoparticles was observed. Likewise, decreasing the Mw of chitosan induced a minor reduction of the particles sizes.

Similar observations reported by Gan *et al*.[38] found most prominent factor influencing the particle size was the concentration of chitosan solution. Unfortunately, the latter aspect was not screened in the present work as its desired diameter for targeted application was reached with the tested concentration. A result of its small size, the loading of AZT doesn't seem to affect the diameter of the nanoparticles because it remained in a similar range for AZT-loaded nanoparticles as for the unloaded ones prepared in the same conditions.

The resulting nanoparticles were also examined by FT-IR, mainly to confirm the occurrence of crosslinking and loading of AZT. Recorded spectra for neat unloaded nanoparticles and those loaded with AZT are shown in Figure 2(b) and 2(c) respectively. The spectrum of CS is also given in Figure 2(a) as reference. The CS matrix presented some characteristic peaks: at 3400 cm^{-1} attributed to the $–NH_2$ and –OH groups stretching vibration and intermolecular hydrogen bonding; at 1597 cm^{-1} and 1660 cm^{-1} ascribed to the N-H bending and primary amide groups, respectively.[40] After crosslinking with TPP, the peak at 1597 cm^{-1} shifted to 1533 cm^{-1} and the peak at 1660 cm^{-1} disappeared along with the appearance of a new sharp peak at 1630 cm^{-1}.

These differences are related to the association between phosphate and ammonium ions,[41] attesting the success of ionic- crosslinking. When loaded with AZT, the broad peak centered at 3400 cm^{-1} shifted toward 3431 cm^{-1} due to contribution of OH groups belonging to AZT stretching and intermolecular hydrogen bonds associated to OH groups of CS. The characteristic absorption peak of AZT at 2119 cm^{-1} corresponding to the azido group ($–N_3$) was also present but shifted to 2110 cm^{-1}.[42] These results indicate that AZT was successfully loaded into the CS nanoparticles.

Loading Capacity (LC) and Encapsulation Efficiency (EE) of AZT. The LC and EE of the CS nanoparticles with respect to AZT were evaluated at different conditions by varying the Mw of CS, TPP concentration, and initial concentration of AZT (Table 1). Nanoparticles made with CS having very small or very high molecular weight appeared to have a restricted ability to load and encapsulate AZT. It seems that there is an optimum molecular weight where CS chains are more flexible and able to entangle and entrap AZT molecules within their structure.[43] In fact nanoparticles made with CS of 63 kDa present the highest EE and LC (13.53 and 5.4 respectively) while they were around 7.25 and 2.87 for 13 kDa and 3.35 and 1.33 for 125 kDa. The increase of the TPP concentration led to a reduction of LC and EE of the nanoparticles. In fact, by increasing TPP concentration, the crosslinking density was augmented inducing a decrease in free volume within the nanoparticles thus resulting in a decrease in loading capacity. Also, the number of junction sites available to interact with AZT was reduced when the crosslinking increased, thereby impacting negatively the EE of the nanoparticles. Obviously, the prominent factor that influences the LC and EE of AZT within CS nanoparticles was the initial concentration of AZT itself. As expected, the increase of the initial concentration of AZT led to an enhancement of AZT-EE and LC until the association of AZT with CS reached saturation and then EE and LC drop.

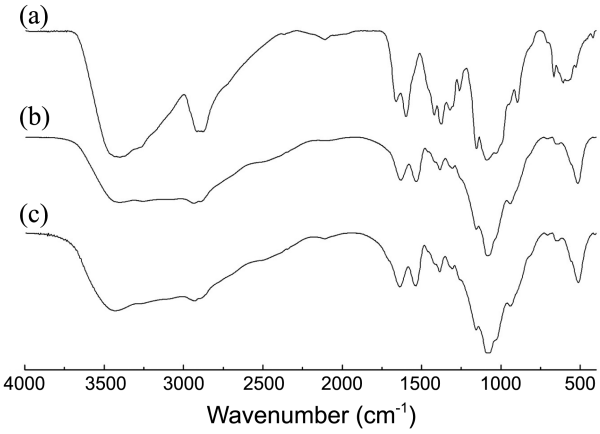

Figure 2. FT-IR spectra of chitosan (a), neat chitosan nanoparticles (b) and chitosan nanoparticles loaded with AZT (c) (conditions: Mw = 125 kDa, TPP/CS = 1.6 and 1 mg/mL as an initial concentration of AZT).

Table 1. Encapsulation efficiency and loading capability of chitosan nanoparticles measured at different conditions

	EE (%)	LC (%)
Mw of Chitosan (kDa)[a]		
13	7.25	2.87
63	13.53	5.4
TPP concentration (mg/mL)[b]		
2.5	7.80	3.11
5	7.04	2.81
10	3.35	1.33
AZT initial concentration (mg/mL)[c]		
1	3.35	1.33
2	7.94	6.34
4	3.54	5.65

[a]realized at AZT initial concentration of 1 mg/mL and TPP/CS ratio of 1.6. [b]realized with Mw of chitosan of 125 kDa and AZT initial concentration of 1 mg/mL. [c]realized with Mw of chitosan of 125 kDa and TPP/CS ratio of 1.6.

***In vitro* Release of AZT Loaded Chitosan Nanoparticles.** The release of AZT from different CS-based nanoparticles was investigated under simulated conditions that closely approximated physiological environment, *ca*. PBS (phosphate buffered saline). *In vitro* release behavior of AZT was affected by almost all parameters tested for the preparation of CS-based nanoparticles. All release profiles of nanoparticles were similar and exhibited a partial burst release in the first 1 to 2 h and then a slower release rate took place at different rates. The AZT could be associated to the nanoparticles in three different states: (i) at the surface of the nanoparticles, (ii) in the core as an irreversible complex with chitosan, or

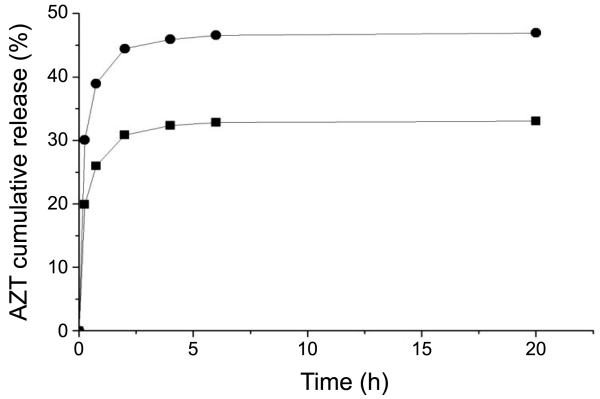

Figure 3. The influences of chitosan MW on AZT release behaviour (● 13 and ■ 63 kDa) (conditions: TPP/Cs ratio of 1.6 and AZT initial concentration of 1 mg/mL).

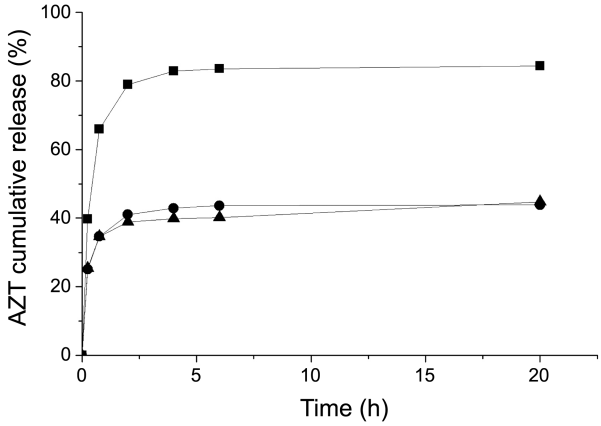

Figure 4. The influences of the TPP concentration on AZT release behaviour (● 2.5, ▲ 5 and ■ 10 mg/mL) (conditions: Mw of CS of 125 kDa and AZT initial concentration of 1 mg/mL).

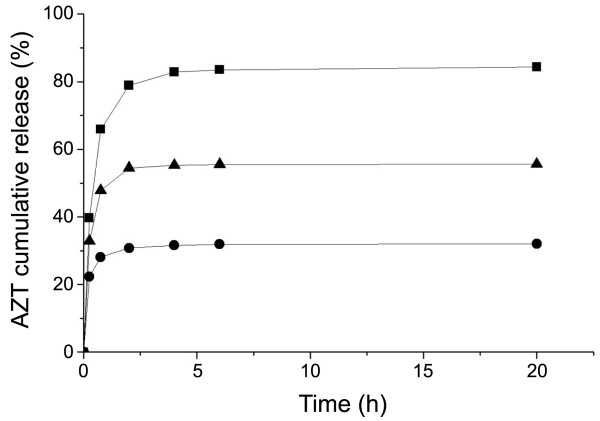

Figure 5. The influences of AZT initial concentrations on it release behavior (■, 1 ●, 2 ▲ 4 mg/mL) (conditions: Mw of CS of 125 kDa and TPP/CS ratio of 1.6).

(iii) in the core as a reversible complex with chitosan. In all cases, the fast release was ascribed to molecules located close to the nanoparticle surface that could easily diffuse out in the initial incubation time. However, molecules forming reversible complexes with CS and located at the core of the nanoparticles take more time to diffuse out while those irreversibly associated with CS remain in the nanoparticle (the reason why the whole amount of loaded AZT is not released). Figure 3 shows the influence of CS molecular weight on the release behavior, the release from nanoparticles made with 13 kDa CS was very fast as leveled off around 44% in the first 2-3 h while it reached only 32% in the case of that prepared with 63 kDa CS. This peculiar behavior is related to the AZT association/complexation in conjunction with the gelation mechanism as previously ascribed for the LE and EE.

Indeed, Small CS (13 kDa and DA = 8%) molecules seem, most probably, to associate with AZT molecules more in reversible complexes. In contrary CS chains with medium molecular weights (63 kDa and DA = 8%) have the ability to entrap AZT molecules within their free volume cavities in both reversible and irreversible complexes as similarly reported by Xu and Du for the release for even larger molecules *ca*. bovine serum albumin (Xu & Du, 2003). A slower release took place afterward at a similar rate for all molecular weights, likely associated with the release of AZT molecules present deeper within the nanoparticle structure. Higher Mw of chitosan with the same DA provides more compact nanoparticles, so lower permeability of nanoparticles surface results in slow release rate. Figure 4 shows the effect of TPP concentration on AZT release from CS-based nanoparticles in PBS. Again, a quick release (39-79%) during the 2-3 first h was observed, suggesting that some AZT was localized at the surface of the nanoparticles. The highest extent of release, 84% after 20 h incubation, was observed for the formulation prepared with a concentration of 10 mg/mL (TPP/CS ratio of 1.6) in comparison with the 44% observed for formulations made with 5 and 2.5 mg/mL TPP (TPP/CS ratios of 0.8 and 0.4 respectively) that show quite similar profiles. This observation was associated with the morphology of nanoparticles, which was influenced by the crosslinking density.

In fact, higher TPP/CS ratio led to higher crosslinking density and consequently more compact structures, hence most of the entrapped molecules were located at the surface and diffused outward easily and quickly. The AZT initial concentration influenced the release profiles (Figure 5). With the change of AZT concentration as 1, 2 and 4 mg/mL, the release percentage of AZT after 2 h incubation was around 79%, 31%, and 54%, respectively. As stated earlier, AZT could be associated to the nanoparticles in three different states: (i) at the surface of the nanoparticles (AZT initial concentration = 1 mg/mL), (ii) in the core as an irreversible complex with chitosan (AZT initial concentration = 2 mg/mL), or (iii) in the core as a reversible complex with chitosan (AZT initial concentration = 4 mg/mL). The repartition of the AZT between these three states depends strongly on the initial AZT concentration. Amount and repartition of the AZT inside nanoparticles influence the release rate.

AZT release rate was found to be higher in the formulation of (initial AZT concentration of 1 mg/mL, 125 kDa and TPP/CS ratio of 1.6), when compared to others AZT loaded

formulations. These results indicated that these nanoparticles (AZT initial concentration of 1 mg/mL, 125 kDa of chitosan and TPP/CS ratio of 1.6) are the best a promising carrier system for controlled delivery of AZT as *anti*-HIV drug.

Conclusions

In this work we demonstrate the feasibility of using chitosan-based nanoparticles for the encapsulation and release of AZT, an *anti*-HIV drug. Chitosan nanoparticles loaded with AZT were successfully prepared by gelation of chitosan with TPP by ionic cross-linking and characterized for controlled drug delivery applications. The properties of nanoparticles in term of their morphology, loading capacity and encapsulation efficiency depended mainly on chitosan molecular characteristics and the conditions of preparation. Moreover release rates of AZT from chitosan-based nanoparticles were influenced by chitosan, but effects of the initial amount of AZT and TPP concentration on AZT release were clearly dominant. The *in vitro* release studies showed that after an initial burst, all AZT-loaded nanoparticles provided a continuous and slow release. In conclusion, chitosan-based nanoparticles could be used as carrier for controlled AZT release. The present results reveal that there are possibilities to modulate the loading and release rate of AZT by adjusting the concentration of AZT as well as the preparation conditions and molecular features of chitosan. The physicochemical and biological properties of chitosan particularly being a mucoadhesive polymer can be considered a positive aspect for the delivery of AZT. More detailed work is, however, necessary to study more in depth the molecular features of chitosan especially the acetylation aspect. To determine the degree of deacetylation threshold beyond which better encapsulation and release may appear in order to draw a clear-cut correlation between molecular features of chitosan and properties of nanoparticles. In vivo studies are also to be considered.

Acknowledgments. The publication cost of this paper was supported by the Korean Chemical Society.

References

1. Broder, S.; Mitsuya, H.; Yarchoan, R.; Pavlakis, G. N. *Ann. Intern. Med*. **1990**, *113*, 604.
2. Klecker, R. W., Jr.; Collins, J. M.; Yarchoan, R.; Thomas, R.; Jenkins, J. F.; Broder, S.; Myers, C. E. *Clin. Pharmacol. Ther.* **1987**, *41*, 407.
3. Mitsuya, H.; Yarchoan, R.; Broder, S. *Science* **1990**, 1533.
4. Yarchoan, R.; Weinhold, K.; Lyerly, H. K.; Gelmann, E.; Blum, R.; Shearer, G.; Mitsuya, H.; Collins, J.; Myers, C.; Klecker, R.; Markham, P.; Durack Lehrman, S. N.; Barry, D.; Fischl, M.; Gallo, R.; Bolognesi, D.; Broder, S. *The Lancet*. **1986**, *327*, 575.
5. Palombo, M. S.; Singh, Y.; Sinko, P. J. *J. Drug. Deliv. Sci. Technol.* **2009**, *19*, 3.
6. Shahiwala, A.; Amiji, M. M. *J. HIV Ther.* **2007**, *1*, 49.
7. Vyas, T. K.; Shah, L.; Amiji, M. M. *Expert. Opin. Drug. Deliv.* **2006**, *3*, 613.
8. Bajaj, A.; Desai, M. *Pharma. Times* **2006**, *38*, 12.
9. Hans, M. L.; Lowman, A. M. *Curr. Opin. Solid State Mater Sci*. **2002**, *6*, 319.
10. Soppimath, K. S.; Aminabhavi, T. M.; Kulkarni, A. R.; Rudzinski, W. E. *J. Control. Release* **2001**, *70*, 1.
11. Kumar, M. N. V. R.; Muzzarelli, R. A. A.; Muzzarelli, C.; Sashiwa, H.; Domb, A. J. *Chem. Rev.* **2004**, *104*, 6017.
12. Felt, O.; Buri, P.; Gurny, R. *Drug. Dev. Ind. Pharm.* **1998**, *24*, 979.
13. Paul, W.; Sharma, C. P. *STP Pharma. Sciences* **2000**, *10*, 5.
14. Rinaudo, M. *Prog. Polym. Sci.* **2006**, *31*, 603.
15. Kean, T.; Thanou, M. *Adv. Drug. Deliver Rev.* **2010**, *62*, 3.
16. He, P.; Davis, S. S.; Illum, L. *Int. Journal Phar.* **1998**, *166*, 75.
17. Lehr, C. M.; Bouwstra, J. A.; Schacht, E. H.; Junginger, H. E. *Int. J. Pharm*. **1992**, *78*, 43.
18. Porporatto, C.; Bianco, I. D.; Correa, S. G. *J. Leukoc. Biol.* **2005**, *78*, 62.
19. Van der Lubben, I. M.; Verhoef, J. C.; van Aelst, A. C.; Borchard, G.; Junginger, H. E. *Biomaterials* **2001**, *22*, 687.
20. Yamamoto, H.; Kuno, Y.; Sugimoto, S.; Takeuchi, H.; Kawashima, Y. *J. Control. Release* **2005**, *102*, 373.
21. Agnihotri, S. A.; Mallikarjuna, N. N.; Aminabhavi, T. M. *J. Control. Release* **2004**, *100*, 5.
22. Prabaharan, M.; Mano, J. F. *Drug. Deliv.* **2004**, *12*, 41.
23. Ciofani, G.; Raffa, V.; Menciassi, A.; Dario, P. *Biomed. Microdevices* **2008**, *10*, 131.
24. De Campos, A. M.; Sánchez, A.; Alonso, M. J. *Int. J. Pharm*. **2001**, *224*, 159.
25. Dube, A.; Nicolazzo, J. A.; Larson, I. *Eur. J. Pharm. Sci*. **2010**, *41*, 219.
26. Huang, X.; Du, Y. Z.; Yuan, H.; Hu, F. Q. *Carbohydr. Polym.* **2009**, *76*, 368.
27. Janes, K. A.; Fresneau, M. P.; Marazuela, A.; Fabra, A.; Alonso, M. J. *J. Control. Release* **2001**, *73*, 255.
28. Katas, H.; Alpar, H. O. *J. Control. Release* **2006**, *115*, 216.
29. Mitra, S.; Gaur, U.; Ghosh, P. C.; Maitra, A. N. *J. Control. Release* **2001**, *74*, 317.
30. Wilson, B.; Samanta, M. K.; Santhi, K.; Kumar, K. P. S.; Ramasamy, M.; Suresh, B. *Nanomedicine* **2010**, *6*, 144.
31. Rhazi, M.; Desbrières, J.; Tolaimate, A.; Alagui, A.; Vottéro, P. *Polym. Int*. **2000**, *49*, 337.
32. Tolaimate, A.; Desbrières, J.; Rhazi, M.; Alagui, A.; Vincendon, M.; Vottero, P. *Polymer.* **2000**, *41*, 2463.
33. Broussignac, P. *Chimie Industrielle et Genie Chimique.* **1968**, *99*, 1241.
34. Lavertu, M.; Xia, Z.; Serreqi, A. N.; Berrada, M.; Rodrigues A.; Wang, D.; Buschmann, M. D.; Gupta, A. *Journal of Pharmaceutical and Biomedical Analysis* **2003**, *32*, 1149.
35. Rinaudo, M.; Milas, M.; Dung, P. L. *Int. J. Biol. Macromol.* **1993**, *15*, 281.
36. Banerjee, T.; Mitra, S.; Kumar, Singh, A.; Kumar Sharma, R.; Maitra, A. *Int. J. Pharm.* **2002**, *243*, 93.
37. Dudhani, A. R.; Kosaraju, S. L. *Carbohydr. Polym.* **2010**, *81*, 243.
38. Gan, Q.; Wang, T.; Cochrane, C.; McCarron, P. *Colloids Surf. B Biointerfaces* **2005**, *44*, 65.
39. Huang, H.; Yang, X. *Biomacromolecules* **2004**, *5*, 2340.
40. Duarte, M. L.; Ferreira, M. C.; Marvão, M. R.; Rocha, J. *Int. J. Biol. Macromol.* **2002**, *31*, 1.
41. Knaul, J. Z.; Hudson, S. M.; Creber, K. A. M. *J. Appl. Polym. Sci*. **1999**, *72*, 1721.
42. Wannachaiyasit, S.; Chanvorachote, P.; Nimmannit, U. *AAPS Pharm. Sci. Tech.* **2008**, *9*, 840.
43. Xu, Y.; Du, Y. *Int. J. Pharm.* **2003**, *250*, 215.